Pinning of vortices by parallel twin boundaries in superconducting single crystals

E. B. Sonin
Ioffe Physical Technical Institute, St. Petersburg 194021, Russia
(Received 4 May 1993; revised manuscript received 25 June 1993)

Pinning of a vortex array by parallel twin boundaries is theoretically investigated. The phase diagram, the magnetic torque, and the resistance in the external magnetic field rotated in the *a-b* plane are studied. In a dense vortex array the collective effects due to long-range interaction between vortices become of importance. They confine the distortion of the vortex array near the twin boundaries to distances of order of the intervortex spacing, thereby suppressing the influence of the twin boundaries on the whole vortex-array pattern when the magnetic field is increased. Nevertheless, the critical angle between the magnetic field and the twin boundaries, at which pinning onset takes place, weakly depends on the magnetic-field value, in agreement with experiment. It is shown that measurement of the Hall resistance is an effective tool to study pinning by twin boundaries.

I. INTRODUCTION

The interaction between vortices and twin boundaries strongly influences the properties of the high-T_c superconductors. It is usually believed that the order parameter is suppressed at the twin boundary.[1] As a result, the twin boundary attracts vortices, i.e., *pins* them. It has been confirmed by decoration experiments on the visualization of vortices.[2,3] Also, measurements of resistivity have been performed in $YBa_2Cu_3O_{7-\delta}$ single crystals which contained the twin planes oriented in only one direction.[4–6] They have revealed drastic changes of resistivity when the external dc magnetic field was aligned along the twin boundaries. It was interpreted as due to pinning of vortices by twin boundaries. Blatter, Rhyner, and Vinokur[7] have developed the theory in which pinning by twin boundaries occurred when the angle between the dc magnetic field and the twin boundaries did not exceed some critical value. They have derived the expression for the critical angle at low magnetic fields when the vortex interaction is negligible and estimated the effect of the vortex interaction for arbitrary magnetic field using the tilt modulus of the vortex array. They concluded that the increasing magnetic field suppressed the pinning by twin boundaries and reduced the critical angle. It did not agree with observed weak dependence of the critical angle on the magnetic field.[6]

In the present paper, pinning by twin boundaries is studied in terms of continuum electrodynamics for type-II superconductors which takes into account the elastic vortex-line tension, but neglects the shear rigidity from the crystalline order of the vortex array. In the past this phenomenological description was developed in the hydrodynamics of rotating He II in works by Hall,[8] Bekarevich and Khalatnikov,[9] and Andronikashvili *et al.*[10] (see also Ref. 11). Its application to type-II superconductors was initiated by Abrikosov, Kemoklidze, and Khalatnikov[12] and worked out by Mathieu and Simon.[13] A similar theory, which was called two-mode electrodynamics, has been recently used to calculate the surface impedance of the type-II superconductor in the mixed state.[14] A central point of this theory is that there are two space scales (two modes) for penetration of ac perturbation from the surface into the superconductor with a dense vortex array: The first one is of the order of the London penetration length or the skin-layer width and was well known earlier; the second scale, which will be called the distortion screening length, is specific for type-II superconductors with elastic vortex arrays. For the case of a dense vortex array, the latter is of the order of the intervortex distance in the low-frequency limit. Earlier screening of vortex-array distortions near sample boundaries was analyzed for rotating superfluids.[15,11] There it was called the superfluid Ekman layer width. It governs the penetration of the perturbation from the slowly oscillating solid surfaces which were investigated in the classic pile-of-disk experiments in rotating He II. The superfluid Ekman layer is crucial for interpretation of recent observations of the slow collective vortex mode in the *B* phase of ^3He.[16]

In the present paper, we shall show that the distortion screening length is important also for pinning by twin boundaries. At the distance of the distortion screening length from the twin boundary, the vortex array transforms from the pattern dictated by the twin boundary to that determined by the external magnetic field. Thus the effect of twin boundaries is confined to the distortion screening length which is decreasing when the external magnetic field is increasing, but the value of the critical angle weakly depends on the magnetic fields contrary to the result of Ref. 7. Screening of vortex-array distortions from the boundary perturbations is tightly connected with the long-range interaction of vortices, as the Debye screening due to the long-range Coulomb interaction in a plasma.

On the basis of the developed theory, the phase diagram of the twinned superconductor is studied for a simple slab geometry in the external magnetic field parallel to the slab. In many aspects the pinning of vortices by parallel twin boundaries is similar to the intrinsic pinning in the space between the Cu-O layers.[17–20] However, there are important differences: (i) Contrary to intrinsic

pinning, the width of the twin boundary may be neglected compared to the spacing between them; (ii) in the case of intrinsic pinning, the distance between the pinning plane is of atomic scale and the distortion screening discussed in the present paper is not relevant then. Thus the phase diagram of the vortex array pinned by the twin boundaries reminds that obtained for the case of the intrinsic pinning[19] only at small spacing between the twin boundaries. The distortion screening, which suppresses the effect of pinning, strongly influences the phase diagram.

The plan of the paper is the following. In Sec. II pinning of a single vortex line is considered. Here the ideas of Blatter, Rhyner, and Vinokur[7] are presented and developed. In Sec. III the general aspects of the continuum electrodynamics of the type-II superconductor in the mixed state are discussed: the free energy, the phase, and the currents and the procedure of averaging over the periodic twin structure of the fields involved. The results of this section are used in Sec. IV to obtain the phase diagram in the external magnetic field rotating in the a-b plane for the vortex array of small, but finite vortex density. In Sec. V the continuum model is applied to find the vortex pattern and the magnetic field for an arbitrary dense vortex array. The effect of vortex interaction on the phase diagram is analyzed. The magnetic torque as a function of the angle between the external magnetic field and the twin planes is calculated in Sec. VI. The effect of twin-boundary pinning on the resistivity is discussed in Sec. VII in terms of the phenomenological model which assumes the dynamic parameters of the vortex inside the twin domain and that trapped by the twin boundary to be known. Special attention is devoted to the Hall resistance, which is an effective probe of trapping of vortices by the twin boundaries.

II. PINNING OF A SINGLE VORTEX LINE

Following Blatter, Rhyner, and Vinokur,[7] let us consider the pinning by twin boundaries in a simplified model which neglects interaction of vortex lines. We assume that the twin boundaries are parallel with spacing d and normal to the a-b plane (see Fig. 1) as in the experiment.[4-6] The shape of the vortex line is governed by the line tension, which is the energy per unit length of the vortex line,

$$\varepsilon=\left[\frac{\Phi_0}{4\pi\lambda}\right]^2\ln\frac{r_0}{r_c}=\frac{\Phi_0}{4\pi}H^* \ . \tag{1}$$

Here $\Phi_0=hc/2e$ is the magnetic-flux quantum, h is the Planck constant, e is the electron charge, c is the light velocity, r_c is the vortex-core radius, and r_0 is the outer radius of the vortex. In the limit of low fields close to H_{c1} (a low-density vortex array), the radius r_0 is equal to the London penetration depth λ and correspondingly the field H^* coincides with the lower critical field H_{c1}. But at higher magnetic fields r_0 is equal to the intervortex distance r_v, which is inversely proportional to $\sqrt{H}$. Thus the characteristic field H^* weakly depends on the magnetic field, and mostly we shall ignore this dependence.

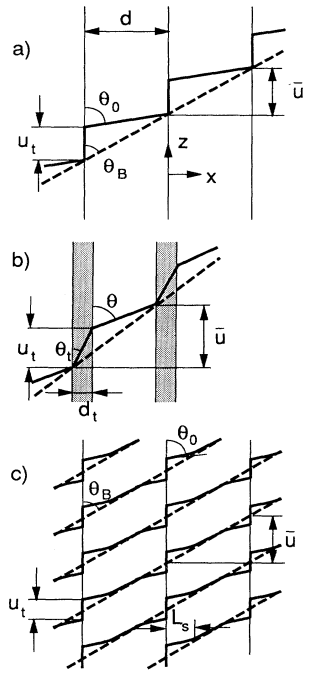

FIG. 1. Pinning of vortices by twin boundaries: (a) a single vortex, infinitely thin twin boundaries (thin solid vertical lines); (b) a single vortex, twin boundaries of finite thickness (grey vertical stripes); (c) a dense vortex array, infinitely thin twin boundaries (thin solid vertical lines). The vortex lines are shown by thick solid lines; their average straightened positions are pictures by thick dashed lines.

Here and thereafter we give all our expressions as if for an isotropic type-II superconductor. However, they are valid for a uniaxial anisotropic layered superconductor if the magnetic field rotates in the a-b plane. In this case the vortex energy does not vary at the rotation, but the vortices themselves are nonaxisymmetric and the penetration depth λ and the core radius r_c are combinations of the penetration depths and the correlation lengths ξ for the a-b plane and the c axis: $\lambda=\sqrt{\lambda_{ab}\lambda_c}$, $r_v=\sqrt{\xi_{ab}\xi_c}$ (see, e.g., Ref. 21).

When the vortex line is aligned along the twin boundary, its line tension ε_t is less than the bulk line tension ε. The difference $\varepsilon-\varepsilon_t$ is responsible for pinning by twin planes. As a result of it, the vortex line becomes a broken line with periodically repeating straight segments: One, of length u_t, adjusts to the twin boundary and the other, of length $\sqrt{(\bar{u}-u_t)^2+d^2}$, is stretched between two neighboring twin boundaries [see Fig. 1(a)]. Here $\bar{u}$ is the displacement of the vortex line along the twin boundary per one period. The vortex energy per one period is

$$E=\varepsilon_t u_t+\varepsilon\sqrt{(\bar{u}-u_t)^2+d^2} \ . \tag{2}$$

Finally, the shape of the vortex line is determined by minimizing the energy in respect to u_t at fixed average slope $\bar{u}/d$:

$$\frac{dE}{du_t}=\varepsilon_t-\varepsilon\frac{\bar{u}-u_t}{\sqrt{(\bar{u}-u_t)^2+d^2}}=0\ . \tag{3}$$

This condition has a simple physical meaning: It is the balance of the line-tension forces in the twin plane for the free and trapped segments of the vortex line in the point of their connection:

$$\varepsilon_t=\varepsilon\cos\theta_0\ . \tag{4}$$

Here θ_0 is the angle between the twin boundary and the free segment of the vortex line which is not trapped, whereas the angle θ_B points out the average direction of the vortex line (see Fig. 1). The vortex line is distorted by the twin-boundary pinning until $\theta_B<\theta_0$. When $\theta_B>\theta_0$ the energy of the vortex line is minimal at $u_t=0$ and the twin boundary does not influence the shape of the vortex line. Thus θ_0 is the critical angle at which the onset of pinning by twin boundaries occurs. The formula $\theta_0=\sqrt{2(\varepsilon-\varepsilon_t)/\varepsilon}$ obtained in Ref. 7 follows from Eq. (4) in the limit of weak pinning when $\varepsilon-\varepsilon_t\ll\varepsilon$.

The boundary condition Eq. (4) has been derived earlier for a superfluid vortex trapped by a thin wire in the theory,[22] developed for the interpretation of the experiment on the precession of the vortex around the wire.[23] Later, we shall see that this condition is not restricted to the case of a single noninteracting vortex and remains also valid for a dense vortex array (high magnetic fields).

It should be pointed out that the onset of the twin-boundary pinning is sharp only if the width of the twin boundary is neglected compared to the distance between boundaries. In a more general model in which the width d_t of the twin boundary is finite, but the line tension does not vary inside the twin boundary, the expression Eq. (2) for the energy must be rewritten as

$$E=\varepsilon_t\sqrt{u_t^2+d_t^2}+\varepsilon\sqrt{(\bar{u}-u_t)^2+(d-d_t)^2}\ , \tag{5}$$

which yields, after minimization in respect to u_t,

$$\varepsilon_t\frac{u_t}{\sqrt{u_t^2+d_t^2}}-\varepsilon\frac{\bar{u}-u_t}{\sqrt{(\bar{u}-u_t)^2+(d-d_t)^2}}=0 \tag{6a}$$

or

$$\varepsilon\cos\theta_t=\varepsilon\cos\theta\ , \tag{6b}$$

where θ is the angle for the segment of the vortex line between the twin boundary and θ_t is that inside the twin boundary [see Fig. 1(b)]. As well as Eq. (4), Eq. (6) is the condition of the balance of the line-tension forces, but now the vortex line trapped by the twin boundary is tilted to it and the angle θ differs from the critical angle θ_0. Thus at finite d_t the onset of pinning is smeared: It is not a sharp phase transition, but a crossover from small values of $u_t\sim d_t/d$ to the region of large u_t in which $\theta\approx\theta_0$.

Using the decoration experiments,[3] Blatter, Rhyner, and Vinokur[7] estimated that $(\varepsilon-\varepsilon_t)/\varepsilon\approx0.03$. Then the resulting critical angle is $\theta_0\approx14°$ in a reasonable agreement with the experiment. However, as mentioned above, the experimental critical angle weakly depends on the magnetic field,[6] which contradicts the prediction by Blatter, Rhyner, and Vinokur, but agrees with the theory developed in the following sections of the present paper.

III. CONTINUUM MODEL OF THE TYPE-II SUPERCONDUCTOR IN THE MIXED STATE

At a finite density of vortex lines, it is necessary to supplement the energy of the line tension, Eq. (2), by the energy of the magnetic fields induced by vortices. The general expression for the free energy of the superconductor in the mixed state in the London model averaged over the vortex-array cell is

$$\begin{aligned}F&=\int d\mathbf{r}\left\{\frac{h(\mathbf{r})^2}{8\pi}+\frac{2\pi\lambda^2}{c^2}j(\mathbf{r})^2+\varepsilon n_v\right\}\\&=\int d\mathbf{r}\left\{\frac{h(\mathbf{r})^2}{8\pi}+\frac{2\pi\lambda^2}{c^2}j(\mathbf{r})^2+\frac{H^*\mathcal{B}}{4\pi}\right\}\ .\end{aligned} \tag{7}$$

Here $\mathbf{h}(\mathbf{r})=[\nabla\times\mathbf{A}]$ is the magnetic field and

$$\mathbf{j}(\mathbf{r})=\frac{c}{4\pi\lambda^2}\left[\frac{\Phi_0}{2\pi}\nabla\phi-\mathbf{A}\right] \tag{8}$$

is the current density averaged over the vortex-array cell; n_v is the two-dimensional vortex density equal to the number of vortices per unit area in the plane normal to the vortex lines. It is useful to introduce the vector of the vortex induction $\mathcal{B}$ with the magnitude $\mathcal{B}=\Phi_0 n_v$ and the direction tangent to the vortex lines. For an uniform vortex array, the vortex induction coincides with the magnetic induction $\mathbf{B}$, which is equal to the average magnetic field $\langle\mathbf{h}(\mathbf{r})\rangle$ by definition, but for a deformed vortex array the difference between the vortex induction $\mathcal{B}$ and the magnetic induction $\mathbf{B}=\langle\mathbf{h}(\mathbf{r})\rangle$ is important:[14] It incorporates the long-range interaction in the vortex array at scales shorter than the London penetration depth, but much longer than the intervortex distance $r_v\sim\sqrt{\Phi_0/\mathcal{B}}$. The third term $\propto n_v\propto\mathcal{B}$ in Eq. (7) is the contribution of the circular currents $\propto1/r$ around the vortex lines (r is a distance from a vortex line) which was not incorporated by the energies of the averaged fields and currents [the two first terms in Eq. (7)]. This contribution is responsible for the vortex-line tension given by Eq. (1). In our theory we assume that the logarithm in this expression is large and neglect the shear modulus of the vortex array: Its energy depends only on the vortex density. This approximation is similar to that used for rotating superfluids.[8–11] For type-II superconductors, this approach was applied in Ref. 12–14.

In the presence of vortices, the phase $\phi(\mathbf{r})$ of the order parameter is a multivalued function and the phase circulation around a closed path is determined by a number of vortices surrounded by the path:

$$\frac{\Phi_0}{2\pi}\oint d\mathbf{l}\cdot\nabla\phi=\int d\mathbf{s}\cdot\mathcal{B}\ , \tag{9}$$

where $\int d\mathbf{s}$ is the integration over the surface encircled by the closed path. It means that the gradient of the multivalued phase is not curl free and is connected with the vortex induction:

$$\frac{\Phi_0}{2\pi}[\nabla\times\nabla\phi]=\mathcal{B}\ . \tag{10}$$

Then one obtains, from Eq. (8),

$$\frac{4\pi}{c}[\nabla\times\lambda^2\mathbf{j}]=\mathcal{B}-\mathbf{h}\ . \tag{11}$$

The equation remains valid even if λ varies in space.

Now let us apply these general relations to our periodic twin structure. By averaging Eq. (11) over the period, one obtains that the average vortex induction and the average magnetic field coincide. The latter is the magnetic induction by definition, i.e.,

$$\mathbf{B}=\langle\mathbf{h}\rangle=\langle\mathcal{B}\rangle\ . \tag{12}$$

Note that now we are averaging $\mathbf{h}$ and $\mathcal{B}$ over the twin structure, but $\mathbf{h}$ and $\mathcal{B}$ themselves have already been averaged over the vortex-array cell.

In our geometry the x components of the vortex induction and the magnetic field do not vary in space since both are divergent free: $B_x=h_x=\mathcal{B}_x$. But the z components of $\mathbf{h}$ and $\mathcal{B}$ are different. In our limit of very thin twin boundaries, the magnetic field remains continuous and only the integral over the space between twin boundaries contributes to its average value:

$$B_z=\frac{1}{d}\int_0^d h_z(x)dx\ . \tag{13}$$

Contrary to it, the z component of the vortex induction $\mathcal{B}_z=B_x dz(x)/dx$ has a singular contribution from a twin boundary where the vortex line is parallel to the twin plane (the yz plane): $dz/dx\to\infty$. Here $z(x)$ describes the shape of the vortex line in the xz plane, which is shown in Fig. 1. The singular contribution to the integral of the vortex induction is of the δ-function form and is proportional to the length u_t of the vortex line trapped by a twin boundary. Then the condition on the z component $\mathcal{B}_z$ of the vortex induction is

$$B_z=B_x\frac{u_t}{d}+\frac{1}{d}\int_0^d\mathcal{B}_z(x)dx\ . \tag{14}$$

The approach developed is a mean-field theory neglecting fluctuations which are shown to be important for Bi- and Tl-based layered superconductors with a weaker coupling between layers than for Y-Ba-Cu-O materials.[24] But even in Y-Ba-Cu-O materials for which the pinning by twin boundaries has been revealed, the fluctuations may play a considerable role for vortex arrays of low density or small angles between vortices and twin boundaries when the number of vortex segments inside the twin domains is rather small. This problem requires a further analysis. However, it is difficult to expect a pronounced effect of fluctuations on the properties discussed in the present paper (the phase diagram, the magnetic torque, the resistance). More promising is to search for the fluctuation effects in the NMR and the muon-spin-resonance experiments as discussed in Ref. 25.

IV. PHASE DIAGRAM IN THE EXTERNAL MAGNETIC FIELD IN THE MODEL OF ISOLATED VORTICES

The model of isolated vortex lines is valid until the spacing d is small enough and the magnetic field $\mathbf{h}$ does not vary in space and thus is equal to the magnetic induction everywhere ($\mathbf{B}=\mathbf{h}$). The z component $\mathcal{B}_z$ of the vortex induction is equal to that of the magnetic induction only on average ($\langle\mathcal{B}_z\rangle=B_z$), but between the twin boundaries it does not vary: $\mathcal{B}_z=B_x\cot\theta_0$ and $\mathcal{B}=B_x/\sin\theta_0$. Thus the magnetic field which incorporates interaction between the vortices has no effect on the shape of the vortex lines in the case discussed. Inside the twin boundary where the vortex line is vertical, $\mathcal{B}_z$ is infinite and according to Eq. (14) in the limit $d_t\to 0$ we obtain

$$\int_{-d_t/2}^{d_t/2}\mathcal{B}_z dx=B_x u_t=B_z d-\int_0^d\mathcal{B}_z dx$$
$$=(B_z-B_x\cot\theta_0)d\ . \tag{15}$$

Then the free-energy density averaged over the structure period is

$$f=\frac{F}{V}=\frac{B^2}{8\pi}+\frac{H^*B_x}{4\pi\sin\theta_0}+\frac{H_t^*(B_z-B_x\cot\theta_0)}{4\pi}\ , \tag{16}$$

where three terms correspond to the magnetic energy and the line-tension energy of the vortex segments between ($\propto H^*$) and inside ($\propto H_t^*$) of the twin boundaries. Since $H_t^*=H^*\cos\theta_0$, the free-energy density is

$$f=\frac{B^2}{8\pi}+\frac{H^*(B_x\sin\theta_0+B_z\cos\theta_0)}{4\pi}\ . \tag{17}$$

To discuss the phase diagram of a sample in an external magnetic field, one should know its demagnetizing factors. We shall restrict ourselves by a simple geometry of a slab of large area parallel to the a-b plane. Then the external magnetic field parallel to the slab coincides with the thermodynamic field $\mathbf{H}$ with the components

$$H_x=4\pi\frac{\partial f}{\partial B_x}=B_x+H^*\sin\theta_0\ , \tag{18}$$

$$H_z=4\pi\frac{\partial f}{\partial B_z}=B_z+H^*\cos\theta_0\ . \tag{19}$$

These relations refer to the region where the vortex lines are partially trapped by the twin boundaries as in Fig. 1(a), i.e., at $\theta_B>\theta_0$. In the region $\theta_B<\theta_0$, where pinning is not effective, the magnetic induction $\mathbf{B}$ and the magnetic field $\mathbf{H}$ are colinear and their magnitudes are connected by the same relation as in an uniform superconductor:

$$H=B+H^*\ . \tag{20}$$

In addition, there are regions of the full and the partial Meissner states in the $\mathbf{H}$ plane. The former, as usual, corresponds to the absence of vortices at all, i.e., $B=0$, and the magnetic field satisfies the inequalities $H<H_{c1}$ if $\theta_B<\theta_0$ and $H_z<H_{c1}\cos\theta_0$ if $\theta_B>\theta_0$. In the partial Meissner state, the vortices penetrate along twin boundaries, but twin domains remain free from vortices yet; in other words, the vortices are completely locked in the

twin boundaries. Then B_z and H_z satisfy Eq. (19), but instead of Eq. (18), $B_x=0$ and $H_x<H_{c1}\sin\theta_0$.

Summarizing, the phase diagram in the plane of **H** consists of the following regions [see Fig. 2(a)].

(i) Region 1 of the full Meissner state. It is restricted by the circle $|H|=H_{c1}$ and by the horizontal lines $|H_z|=H_{c1}\cos\theta_0$.

(ii) Region 2 of the partial Meissner state which will be called the lock-in phase. It consists of two stripes restricted by vertical lines $|H_x|=H_{c1}\sin\theta_0$ of the lock-in phase transition (LPT) (see Fig. 2) and by the horizontal lines $|H_z|=H_{c1}\cos\theta_0$.

(iii) In region 3 the vortices are tilted in respect to the twin boundaries, but finite segments of them (of length u_t) are trapped by the twin boundaries. This region, which will be called the pinning phase, is restricted by the LPT lines and by the pinning phase transition (PPT) lines $\theta_B=\pm\theta_0$ (see Fig. 2).

(iv) The rest of the **H** plane (region 4) is occupied by the usual mixed state without any effect of the twin boundaries.

Thus the effect of twin boundaries is present in regions 2 and 3 (the lock-in and pinning phases shadowed in Fig. 2).

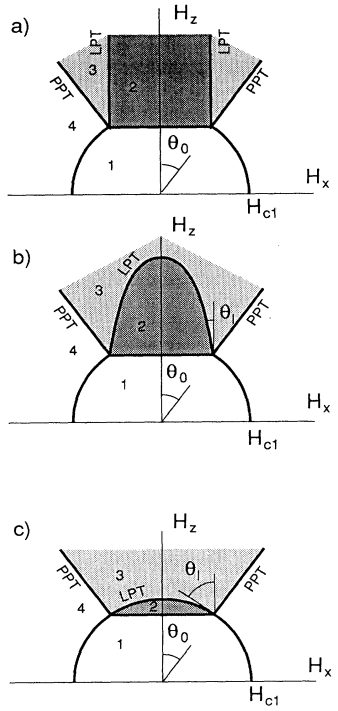

FIG. 2. Phase diagram in the external magnetic field **H** which rotates in the a-b plane (only the upper half of the H_x-H_z plane is shown): (a) the twin domains are thin compared to the London penetration depth ($d\ll\lambda$), and the vortex interaction is neglected; (b) the twin-domain width is comparable with the London penetration depth ($d\sim\lambda$); (c) thick domains ($d\gg\lambda$), the vortex interaction is very strong and reduces the lock-in phase transition (the LPT line) to the transition into the mixed state of the macroscopic twin domain. The phases are (1) the full Meissner state, no vortices; (2) the partial Meissner state, there are vortices confined to the twin boundaries, but the twin domains remain free from vortices (the lock-in phase); (3) the mixed state with partially trapped vortices (the pinning phase); (4) the usual mixed state without any effect of twinning on the vortex-array pattern. Thus the effect of twin-boundary pinning is present in the shadowed regions (2) and (3).

V. CONTINUUM MODEL: THE EQUATIONS FOR THE DISTORTED VORTEX ARRAY

In general, the equations for the vortex array are derived by varying the free energy Eq. (7) with respect to small $\delta\phi$, $\delta\mathbf{A}$, and $\delta\mathbf{u}$. Here the small phase variation $\delta\phi$ is assumed to be single valued and well defined everywhere; then, the variation of the phase yields the continuity equation $\nabla\cdot\mathbf{j}=0$. Variation of the free energy with respect to the electromagnetic vector potential **A** gives the Maxwell equation

$$[\nabla\times\mathbf{h}]=\frac{4\pi}{c}\mathbf{j}\ . \tag{21}$$

In order to obtain the equation of the force balance for the vortex array, we should find a variation of the free energy with respect to the displacements $\delta\mathbf{u}$ of the vortex lines. There is a relation between variations $\delta\mathbf{u}$ and $\delta\mathcal{B}$ which follows from simple geometric arguments and vector identities:

$$\delta\mathcal{B}=-\mathcal{B}\nabla\cdot\delta\mathbf{u}+(\mathcal{B}\cdot\nabla)\delta\mathbf{u}=-[\nabla\times[\mathcal{B}\times\delta\mathbf{u}]]\ . \tag{22}$$

With the help of Eq. (11), one can find the relation between variations $\delta\mathbf{j}$ and $\delta\mathbf{u}$:

$$\frac{4\pi\lambda^2}{c}[\nabla\times\delta\mathbf{j}]=\delta\mathcal{B}=-[\nabla\times[\mathcal{B}\times\delta\mathbf{u}]] \tag{23}$$

or

$$\frac{4\pi\lambda^2}{c}\delta\mathbf{j}=-[\mathcal{B}\times\delta\mathbf{u}]\ . \tag{24}$$

Bearing in mind Eqs. (22) and (24), the variation of the free energy with respect to $\delta\mathbf{u}$ is

$$\delta F_u=\int d\mathbf{r}\left[\frac{4\pi\lambda^2}{c}\mathbf{j}\cdot\delta\mathbf{j}+\frac{H^*}{4\pi\mathcal{B}}\mathcal{B}\cdot\delta\mathcal{B}\right]$$
$$=\int d\mathbf{r}\left[\frac{1}{c}\mathbf{j}\cdot[\delta\mathbf{u}\times\mathcal{B}]+\frac{H^*\mathcal{B}\cdot[\nabla\times[\delta\mathbf{u}\times\mathcal{B}]]}{4\pi\mathcal{B}}\right]\ . \tag{25}$$

After integrating by parts, one obtains the Euler-Lagrange equation for the bulk:

$$\frac{1}{c}[\mathcal{B}\times\mathbf{j}]+\left[\mathcal{B}\times\left[\nabla\times\frac{H^*\mathcal{B}}{4\pi\mathcal{B}}\right]\right]=0\ . \tag{26}$$

In the left-hand side of Eq. (26), the first term is the Lorentz force and the second term is the elastic restoring force from line tension of the vortex lines, both normalized per unit volume. If the bulk equation (26) is satisfied, the variation of the free energy is reduced to the integral over the surface of the superconductor:

$$\delta F_u = \int d\mathbf{S}\cdot\frac{H^*}{4\pi\mathcal{B}}[\mathcal{B}\times[\mathcal{B}\times\delta\mathbf{u}]]$$
$$= -\int d\mathbf{S}\cdot\frac{H^*\mathcal{B}}{4\pi}\left[\delta\mathbf{u}-\frac{\mathcal{B}}{\mathcal{B}}(\mathcal{B}\cdot\delta\mathbf{u})\right], \quad (27)$$

where the differential vector $d\mathbf{S}$ is normal to the boundary surface. By definition, the variation of the free energy with respect to the vortex displacement is a force on the vortex array and the tensor:

$$\sigma_{ik} = \frac{H^*\mathcal{B}}{4\pi}\left[\delta_{ik}-\frac{\mathcal{B}_i\mathcal{B}_k}{\mathcal{B}^2}\right] \quad (28)$$

is the elastic momentum-flux tensor of the vortex array. If there is no force on the vortex array at the superconductor surface, the momentum flux vanishes at the surface and the vector induction; i.e., the vortex lines are normal to the surface. Equations (11), (21), and (26) together with the boundary conditions form a complete set of equations describing the elastic vortex array.

Now let us return to the problem of twin boundaries. The magnetic field $\mathbf{h}$ and the vortex induction $\mathcal{B}$ lie in the xz plane and have only x and z components, whereas the currents are directed along the y axis. All variables depend only on x. Then our electrodynamic equations yield that h_x and $\mathcal{B}_x$ do not vary in space and coincide with the x component of the magnetic induction: $B_x=\mathcal{B}_x=h_x$. After exclusion of the currents from Eqs. (11), (21), and (26), there remain two differential equations for h_z and $\mathcal{B}_z$:

$$h_z-\frac{d}{dx}\left[\lambda^2\frac{dh_z}{dx}\right]=\mathcal{B}_z\ , \quad (29)$$

$$\frac{dh_z}{dx}+\frac{d}{dx}\left[\frac{H^*\mathcal{B}_z}{\mathcal{B}}\right]=0\ . \quad (30)$$

We have also the conditions Eqs. (13) and (14) following from periodicity.

Choosing all displacements of the vortex lines $\delta\mathbf{u}[0,0,\delta z(x)]$ parallel to the z axis, the variation of the free energy given by Eq. (27) may be written as

$$\delta F_u = S\frac{H^*\mathcal{B}_z\mathcal{B}_x}{4\pi\mathcal{B}}[\delta z(d)-\delta x(0)]\ , \quad (31)$$

where S is the twin-boundary area and $\delta z(0)$ and $\delta z(d)$ are variations of the vortex displacements near the twin boundaries at $x=0$ and d. If a segment of the length u_t of the vortex line is pinned by the twin boundary, then the variation of the displacement difference $\delta z(d)-\delta z(0)$ for the segment of the vortex line between the twin boundary (at fixed average slope of the vortex line) shortens the length u_t, i.e., $\delta z(d)-\delta z(0)=-\delta u_t$, and the variation of the free energy of the vortices trapped by the twin boundaries is

$$\delta F_t = S\frac{\mathcal{B}_x}{\Phi_0}\varepsilon_t\delta u_t = -S\frac{\mathcal{B}_x}{\Phi_0}\varepsilon t[\delta z(d)-\delta z(0)]$$
$$= -S\frac{\mathcal{B}_x H_t^*}{4\pi}[\delta z(d)-\delta z(0)]\ , \quad (32)$$

where $\mathcal{B}_x/\Phi_0$ is the number of vortices per unit area of the twin boundary and $H_t^*=4\pi\varepsilon_t/\Phi_0=H^*\cos\theta_0$ is the field determined by the line tension ε_t of the vortex trapped by the twin boundary. The energy is minimal if the sum of the variations $\delta F_u+\delta F_t$ vanishes; it gives the boundary condition for the vortex induction,

$$\frac{\mathcal{B}_z}{\mathcal{B}}=\cos\theta_0\ , \quad (33)$$

where the critical angle θ_0 is determined by the balance of line tensions, Eq. (4). Thus the latter is valid independently of the vortex density. The vortex lines may be trapped by the twin boundaries only if the angle $\theta_B=\arccos B_z/B$ between the magnetic induction $\mathbf{B}=\langle\mathbf{h}(x)\rangle$ and the twin boundary does not exceed the critical angle θ_0. In the dense vortex array, the critical angle θ_0 slightly depends on the magnetic induction because of the logarithmic dependence of the line tension ε on the vortex density, but this dependence is much weaker than that predicted by Blatter, Rhyner, and Vinokur.[7]

The system of the nonlinear equations (29) and (30) together with the conditions Eqs. (13), (14), and (33) yield a general solution of our problem. In the simplified analysis of Secs. II and III, we neglected the space variation of the magnetic field and assumed that free segments of vortices were straight. This is valid until the interaction between vortices is not important. Another case, in which an analytical solution can be obtained, is the region close to the PPT line. There Eqs. (29) and (30) can be linearized in respect to small $\mathcal{B}_z'=\mathcal{B}_z-\mathcal{B}_{z0}$ and $h_z'=h_z-h_{z0}$, where $\mathcal{B}_{z0}=h_{z0}=B_x\cot\theta_0$ are values of $\mathcal{B}_z$ and h_z along the PPT line:

$$h_z'-\lambda^2\frac{d^2h_z'}{dx^2}=\mathcal{B}_z'\ , \quad (34)$$

$$\frac{dh_z'}{dx}+\frac{H^*\sin^3\theta_0}{B_x}\frac{d\mathcal{B}_z'}{dx}=0\ . \quad (35)$$

These equations yield two modes of space variation.[14]

(i) The magnetic field h_z' and the vector induction $\mathcal{B}_z'$ do not vary in space. This is the zero-frequency limit of the skin-layer behavior.

(ii) h_z' and $\mathcal{B}_z'$ vary in space as $\exp(\pm x/L_s)$, where L_s is the vortex-distortion screening length related to the elastic mode of the vortex array[14] and is given by

$$L_s^2=\lambda^2\frac{H^*\sin^3\theta_0}{H^*\sin^3\theta_0+B_x}\ . \quad (36)$$

The superposition of these two modes,

$$h_z'(x)=h_0+h_1\cosh(x/L_s)\ ,$$
$$\mathcal{B}_z'(x)=h_0-\frac{B_x}{H^*\sin^3\theta_0}h_1\cosh(x/L_s)\ , \quad (37)$$

should satisfy the conditions Eqs. (13), (14), and (33). This gives

$$u_t = d\frac{B_z - B_{z0}}{B_x}\frac{H^*\sin^3\theta_0 + B_x}{H^*\sin^3\theta_0 + B_x(d/2L_s)\coth(d/2L_s)} ,$$
$$h_0 = (B_z - B_{x0})\frac{B_x}{B_x + H^*\sin^3\theta_0(2L_s/d)\tanh(d/2L_s)} , \tag{38}$$
$$h_1 = \frac{B_z - B_{z0}}{\cosh(d/2L_s)}\frac{H^*\sin^3\theta_0}{B_x + H^*\sin^3\theta_0(2L_s/d)\tanh(d/2L_s)} .$$

Expanding the free energy and keeping the terms of the second order with respect to $(B_z - B_{z0})$, one obtains the free-energy density in the pinning phase in vicinity of the pinning phase transition:

$$f = \frac{B^2}{8\pi} + \frac{H^*}{4\pi}(B_x\sin\theta_0 + B_z\cos\theta_0) + \frac{(B_z - B_{z0})^2}{8\pi}\frac{H^*\sin^3\theta_0[(d/2L_s)\coth(d/2L_s) - 1]}{H^*\sin^3\theta_0 + B_x(d/2L_s)\coth(d/2L_s)} . \tag{39}$$

The thermodynamic magnetic field **H**, which is equal to the external magnetic field in the parallel slab geometry, is given by

$$H_x = \frac{4\pi}{V}\frac{\partial F}{\partial B_x} = B_x + H^*\sin\theta_0 - (B_z - B_{z0})\frac{H^*\sin^2\theta_0\cos\theta_0[(d/2L_s)\coth(d/2L_s) - 1]}{H^*\sin^3\theta_0 + B_x(d/2L_s)\coth(d/2L_s)} ,$$
$$H_z = \frac{4\pi}{V}\frac{\partial F}{\partial B_z} = B_z + H^*\cos\theta_0 + (B_z - B_{z0})\frac{H^*\sin^3\theta_0[(d/2L_s)\coth(d/2L_s) - 1]}{H^*\sin^3\theta_0 + B_x(d/2L_s)\coth(d/2L_s)} . \tag{40}$$

One may also reverse the obtained formulas and find the magnetic induction **B** as a function of the field **H**:

$$B_x = H_x - H^*\sin\theta_0 + (H_z - H_{z0})\frac{H^*\sin^2\theta_0\cos\theta_0[(d/2L_s)\coth(d/2L_s) - 1]}{-H^*\sin\theta_0\cos^2\theta_0 + H_x(d/2L_s)\coth(d/2L_s)} ,$$
$$B_z = H_z - H^*\cos\theta_0 - (H_z - H_{z0})\frac{H^*\sin^3\theta_0[(d/2L_s)\coth(d/2L_s) - 1]}{-H^*\sin\theta_0\cos^2\theta_0 + H_x(d/2L_s)\coth(d/2L_s)} . \tag{41}$$

This derivation is valid until the shape of vortices slightly deviates from a straight line. It is provided either by small value of $(B_z - B_{z0})$ near the PPT line or by small value of d/L_s when the vortex interaction weakly affects the shape of the vortex lines.

Now one can analyze the effect of the vortex interaction on the phase diagram. Figures 2(a)–2(c) show how the phase diagram varies when the space d between the twin boundaries is increasing and the vortex interaction is becoming more and more important. The position of the PPT line is not affected by the vortex interaction, although the screening of the twin-boundary effect seriously suppresses the contribution from the twin-boundary pinning. (It is easy to check that in the limit of large d/L_s all derived expressions are those for a uniform superconductor expanded near the PPT line.) Contrary to it, the lock-in phase transition is strongly influenced by the vortex-distortion screening. To define the LPT line, one should assume $B_x = 0$ in Eqs. (40) and exclude B_z from them. This yields

$$\tan\theta_l = -\frac{H_x - H_{c1}\sin\theta_0}{H_z - H_{c1}\cos\theta_0}$$
$$= \cot\theta_0[1 - (2L_s/d)\tanh(d/2L_s)] . \tag{42}$$

Here θ_l is the angle in the **H** plane between the z axis and the lock-in line close to the critical point (see Fig. 2). In the limit of small $d \ll L_s \sim \lambda$, the LPT line is nearly vertical as derived above [see Fig. 2(a)], but crosses nevertheless the z axis somewhere beyond the scale of Fig. 2(a) at the value of H_z:

$$H_z = 12\frac{\lambda^2}{d^2}H^*\tan\theta_0\sin\theta_0 . \tag{43}$$

However, at so large H_z the expansion used in the derivation is not exact. Therefore Eq. (43) must be considered as an approximate order-of-magnitude estimation.

In the opposite limit of large $d \gg L_s$, Eq. (42) yields $\theta_l = \pi/2 - \theta_0$, which means that the LPT line is tangent to the circumference $|H| = H_{c1}$. As mentioned above, one may not use Eq. (42) far from the critical point. However, the shape of the LPT line in the limit of very thick twin domains ($d \to \infty$) is clear without any approximation: It should be a segment of the circumference $|H| = H_{c1}$ as shown in Fig. 2(c). Thus the effect of the vortex-distortion screening controlled by the ratio d/L_s changes the LPT line from the vertical straight line [Fig. 2(a)] to the segment of the circumference $|H| = H_{c1}$, which is the transition line at which the vortices begin to penetrate into the macroscopic twin domains [Fig. 2(c)].

It is interesting to compare the effect of the vortex-distortion screening in type-II superconductors with the similar effect in rotating neutral superfluids (^{4}He and ^{3}He). In the neutral superfluid, the penetration depth λ is

infinite and the characteristic field $H^* \to 0$. Also, it should be taken into account that Eq. (36) yields the width of the screening layer in the direction normal to the twin boundary and at the angle $\pi/2-\theta_0$ to the vortex lines. But here we need the screening depth *along* the vortex lines, which is $L_v = L_s/\sin\theta_0$ and according to Eq. (36) is equal to

$$L_v = \lambda \left[\frac{H^*}{\mathcal{B}} \right]^{1/2} = \left[\frac{\Phi_0 \ln(r_v/r_c)}{4\pi\mathcal{B}} \right]^{1/2} = \left[\frac{\ln(r_v/r_c)}{4\pi n_v} \right]^{1/2} . \tag{44}$$

We have obtained the length which exactly coincides with the superfluid Ekman layer width for the rotating superfluids.[11]

VI. MAGNETIC TORQUE FROM PINNING BY TWIN BOUNDARIES

An effective tool to study anisotropy of the type-II superconductors is the measurement of the magnetic torque at rotation of the magnetic field. In the continuum theory, the free energy of a single crystal without twin domains is invariant with respect to rotations in the a-b plane and there is no torque. However, in the presence of parallel twin domains the rotational symmetry is broken and there is a torque which endeavors to orient a sample so that twin domains would be parallel to the magnetic field **H**. The magnitude of the torque per unit volume is given by

$$T = -\frac{1}{V}\frac{\partial F}{\partial \theta_B} = -\frac{1}{V}\frac{\partial G}{\partial \theta_H} = \frac{B_z H_x - B_x H_z}{4\pi} . \tag{45}$$

Here $G = F - V\mathbf{B}\cdot\mathbf{H}$ is the Gibbs thermodynamic potential and θ_B and θ_H are the angles between the twin boundary and the magnetic induction **B** and the magnetic field **H**, respectively.

At first let us consider the simpler case of noninteracting vortex lines. According to Eqs. (18) and (19), the torque for the lock-in phase in which $B_x = 0$ is

$$T = \frac{H_x(H_z - H^*\cos\theta_0)}{4\pi} , \tag{46}$$

and in the pinning phases,

$$T = \frac{H^*(H_z\sin\theta_0 - H_x\cos\theta_0)}{4\pi} = \frac{HH^*}{4\pi}\sin(\theta_0-\theta_H) . \tag{47}$$

On the PPT line, where $\theta_H = \theta_B = \theta_0$, the rotational symmetry is restored and the torque vanishes.

When the distortion screening is important, one must use the formulas derived in Sec. V. Using Eq. (41), the torque as a function of the magnetic field **H** is equal to

$$T = \frac{HH^*}{4\pi}\sin(\theta_0-\theta_H) \times \frac{H - H^*\cos^2\theta_0}{H(d/2L_s)\coth(d/2L_s) - H^*\cos^2\theta_0} . \tag{48}$$

In the limit of $d/L_s \to 0$, Eq. (48) reduces to Eq. (47). In the opposite limit of large d/L_s, distortion screening essentially suppresses the magnetic torque:

$$T = \frac{L_s}{2\pi d} HH^* \sin(\theta_0-\theta_H)\frac{H - H^*\cos^2\theta_0}{H} . \tag{49}$$

The magnetic torque from twin boundaries can explain the magnetic-field-induced orientation of superconducting Y-Ba-Cu-O microcrystals observed with the x-ray diffraction in Ref. 26.

VII. EFFECT OF TWIN BOUNDARIES ON THE RESISTIVITY AND THE HALL EFFECT

Free vortices and those trapped by the twin boundaries are characterized by different dynamic parameters and yield different contributions to resistivity. This has been used for detection of the twin-plane pinning.[4-6] Here we consider the resistivity in different regions of the phase diagram using a simple phenomenological model which assumes the dynamical parameters of vortices inside and outside the twin boundary to be given.

At first, let us derive some general relations for a uniform anisotropic uniaxial conductor in a magnetic field. The anisotropy axis given by the unit vector **m**, which is assumed to be normal to the magnetic induction **B**. Then Ohm's law in the most general form is[27]

$$\mathbf{E} = \rho_l \mathbf{m}(\mathbf{m}\cdot\mathbf{j}) + \rho_t[\mathbf{b}\times\mathbf{m}]([\mathbf{b}\times\mathbf{m}]\cdot\mathbf{j}) + \rho_{Bl}[\mathbf{b}\times\mathbf{m}](\mathbf{m}\cdot\mathbf{j}) - \rho_{Bt}\mathbf{m}([\mathbf{b}\times\mathbf{m}]\cdot\mathbf{j}) + \rho_B\mathbf{b}(\mathbf{b}\cdot\mathbf{j}) \tag{50}$$

or, in the terms of the conductivity,

$$\mathbf{j} = \sigma_l \mathbf{m}(\mathbf{m}\cdot\mathbf{E}) + \sigma_t[\mathbf{b}\times\mathbf{m}]([\mathbf{b}\times\mathbf{m}]\cdot\mathbf{E}) + \sigma_{Bl}[\mathbf{b}\times\mathbf{m}](\mathbf{m}\cdot\mathbf{E}) - \sigma_{Bt}\mathbf{m}([\mathbf{b}\times\mathbf{m}]\cdot\mathbf{E}) + \sigma_B\mathbf{b}(\mathbf{b}\cdot\mathbf{E}) . \tag{51}$$

Here **E** is the electric field, $\mathbf{b} = \mathbf{B}/B$ is a unit vector pointing the direction of the magnetic induction, and $(\rho_l,\rho_t,\rho_{Bl},\rho_{Bt},\rho_B)$ and $(\sigma_l,\sigma_t,\sigma_{Bl},\sigma_{Bt},\sigma_B)$ are the components of the resistance and the conductance, respectively, which are connected by the relations

$$\rho_l = \frac{\sigma_t}{\sigma_l\sigma_t + \sigma_{Bl}\sigma_{Bt}}, \quad \rho_t = \frac{\sigma_l}{\sigma_l\sigma_t + \sigma_{Bl}\sigma_{Bt}} ,$$
$$\rho_{Bl} = -\frac{\sigma_{Bl}}{\sigma_l\sigma_t + \sigma_{Bl}\sigma_{Bt}}, \quad \rho_{Bt} = -\frac{\sigma_{Bt}}{\sigma_l\sigma_t + \sigma_{Bl}\sigma_{Bt}} , \tag{52}$$
$$\rho_B = \frac{1}{\sigma_B} .$$

In experiments they usually measure the components of the electrical field parallel to the current and normal to both the current and the external magnetic field. Since the latter is normal to the anisotropy axis **m** and thereby parallel to the magnetic induction in the slab geometry, these components are

$$E_\parallel = \frac{(\mathbf{E}\cdot\mathbf{j})}{j} = \rho_\parallel j, \quad E_\perp = \frac{(\mathbf{E}\cdot[\mathbf{b}\times\mathbf{j}])}{j} = \rho_\perp j , \tag{53}$$

where the resistances $\rho_\parallel$ and $\rho_\perp$ are

$$\rho_{\parallel}=\frac{1}{j^2}\{\rho_l(\mathbf{m}\cdot\mathbf{j})^2+\rho_t([\mathbf{b}\times\mathbf{m}]\cdot\mathbf{j})^2 +(\rho_{Bl}-\rho_{Bt})(\mathbf{m}\cdot\mathbf{j})([\mathbf{b}\times\mathbf{m}]\cdot\mathbf{j})+\rho_B(\mathbf{b}\cdot\mathbf{j})^2\} ,$$
$$\rho_{\perp}=\frac{1}{j^2}\{\rho_{Bl}(\mathbf{m}\cdot\mathbf{j})^2+\rho_{Bt}([\mathbf{b}\times\mathbf{m}]\cdot\mathbf{j})^2 +(\rho_t-\rho_l)(\mathbf{m}\cdot\mathbf{j})([\mathbf{b}\times\mathbf{m}]\cdot\mathbf{j})\} . \quad (54)$$

For an isotropic conductor, $\rho_l=\rho_t$ (but ρ_B is different because of magnetoresistance) and $\rho_{Bl}=\rho_{Bt}$. Then the transverse component $E_\perp$ presents the Hall effect. However, in an anisotropic case $E_\perp$ includes also a contribution that does not vary when the magnetic field inverts its direction (the "even" Hall effect[28]). Also, the longitudinal component $E_\parallel$ has a term $\propto(\rho_{Bl}-\rho_{Bt})$ odd in the direction of the magnetic field. Both contributions are due to anisotropy.

Now let us apply the relations derived to a type-II superconductor in the resistive mixed state. The electrical field $\mathbf{E}$ is related to the velocity $\mathbf{v}_L$ of the vortex motion by the Josephson relation

$$\mathbf{E}=-\frac{1}{c}[\mathbf{v}_L\times\mathcal{B}] , \quad (55)$$

and the unit vector $\mathbf{b}=\mathcal{B}/\mathcal{B}$ points out the direction of the vortex induction $\mathcal{B}$. The model involves both the flux-flow and creep regimes of vortex motion: The difference between them is supposed to be taken into account by the magnitudes and the dependences of the resistance components. Further, we shall neglect the resistance for currents along the vortices ($\rho_B=0$, $\sigma_B\to\infty$), adopting the simple Lorentz-force concept of vortex motion in which Ohm's law may be presented as the balance of forces acting on the vortex:

$$\frac{\Phi_0}{c}[\mathbf{b}\times\mathbf{j}]=-\frac{\mathcal{B}\Phi_0}{c^2}\{\sigma_t\mathbf{m}(\mathbf{m}\cdot\mathbf{v}_L) +\sigma_l[\mathbf{b}\times\mathbf{m}]([\mathbf{b}\times\mathbf{m}]\cdot\mathbf{v}_L) +\sigma_{Bt}[\mathbf{b}\times\mathbf{m}](\mathbf{m}\cdot\mathbf{v}_L) -\sigma_{Bl}\mathbf{m}([\mathbf{b}\times\mathbf{m}]\cdot\mathbf{v}_L)\} . \quad (56)$$

The Lorentz force in the left-hand side of Eq. (56) is balanced by the friction and transverse forces in the right-hand side which are proportional to the vortex velocity $\mathbf{v}_L$.

In our case the anisotropy axis $\mathbf{m}$ is the c axis and we restrict our analysis by a geometry in which both the current and the magnetic field, as well as vortices, lie in a-b plane, i.e., normal to the anisotropy axis. Then $(\mathbf{m}\cdot\mathbf{j})=0$ and the formulas for the $\rho_\parallel$ and $\rho_\perp$ in the case of straight vortices look as for the isotropic case:

$$\rho_{\parallel}=\rho_t\sin^2(\theta_j-\theta_B),\quad \rho_{\perp}=\rho_{Bt}\sin(\theta_j-\theta_B) , \quad (57)$$

where θ_j is the angle between $\mathbf{j}$ and the twin boundary. The transverse component $E_\perp\propto\rho_\perp$ is to be measured along the c axis.

When the twin-boundary pinning is important and a finite segment of the vortex is trapped by the twin boundary, the vortex velocity $\mathbf{v}_L$ is also determined from the force balance, but the dynamic parameters are different for the trapped and free segments of the vortex lines. Equation (56) refers now to the free segments, but the unit vector $\mathbf{b}=\mathcal{B}/\mathcal{B}$ varies in space. The motion of the distorted vortex line may be described by the y component of the vortex velocity, v_{Ly}, and the z component v_{Lz} describing translation of the free segments along the twin boundaries. We use the balance equations for forces only along the y and z axes: The forces along the x axis include the pinning force which balances all other forces. The Lorentz force has no component on the z axis; the trapped segments of vortices also do not contribute to the balance for the z axis, which is

$$0=\int(\sigma_l b_x^2 v_{Lz}+\sigma_{Bt}b_x v_{Ly})dl . \quad (58)$$

Here the integral expands over the free segment of the vortex line with dl being an infinitesimal element of its length. Bearing in mind that $b_x=\sin\theta(x)$, $b_z=\cos\theta(x)$, and $dx=b_x dl$, where $\theta(x)$ is the angle between the local direction of the vortex line and the z axis, Eq. (58) yields the following relation between the two components of the vortex velocity $\mathbf{v}_L$:

$$\sigma_l\langle\sin\theta(x)\rangle v_{Lz}=-\sigma_{Bt}v_{Ly} , \quad (59)$$

where

$$\langle\sin\theta(x)\rangle=(1/d)\int_0^d\sin\theta(x)dx \quad (60)$$

assumes integration over the space between the twin boundaries.

Now let us consider the balance of forces on the y axis. The total y component of the Lorentz force per one period of the twin structure is

$$(F_L)_y=\int\frac{\Phi_0}{c}[\mathbf{b}\times\mathbf{j}]_y dl=\frac{\Phi_0}{c}\int(b_z j_x-b_x j_z)dl =\frac{\Phi_0}{c}(j_x\bar{u}-j_z d) =\frac{\Phi_0}{c}jL\sin(\theta_j-\theta_B) , \quad (61)$$

where $L=\sqrt{d^2+\bar{u}^2}$. The Lorentz force is balanced by the force

$$(F_R)_y=-\frac{\mathcal{B}\Phi_0}{c^2}\left[\int(\sigma_t v_{Ly}-\sigma_{Bl}b_x v_{Lz})dl+\sigma_{tw}v_{Ly}u_t\right] =-\frac{\mathcal{B}\Phi_0}{c^2}(\sigma_t v_{Ly}\mathcal{L}-\sigma_{Bl}v_{Lz}d+\sigma_{tw}v_{Ly}u_t) . \quad (62)$$

Here $\mathcal{L}=\int dl$ is the length of the distorted free segment of the vortex line between two neighboring twin boundaries and $\sigma_{tw}=1/\rho_{tw}$ is the conductance for the vortex segments trapped by the twin boundaries. Equating the two forces, $(F_L)_y=(F_R)_y$, one obtains the resistances which determine the longitudinal and the transverse components of the electrical field:

$$\rho_{\parallel}=\frac{\sigma_l\langle\sin\theta\rangle}{(\sigma_t\mathcal{L}/d+\sigma_{tw}u_t/d)\sigma_l\langle\sin\theta\rangle+\sigma_{Bl}\sigma_{Bt}}\times\frac{\sin^2(\theta_j-\theta_B)}{\sin\theta_B}\ , \tag{63}$$

$$\rho_{\perp}=-\rho_{\parallel}\frac{\sigma_{Bt}\sin\theta_B}{\sigma_l\langle\sin\theta\rangle\sin(\theta_j-\theta_B)}=\rho_{\parallel}\frac{\rho_{Bt}\sin\theta_B}{\rho_t\langle\sin\theta\rangle\sin(\theta_j-\theta_B)}\ . \tag{64}$$

Now let us apply the expressions derived to some simple cases. If the twin-plane pinning is absent and the vortex lines are straight, then $\langle\sin\theta\rangle=\sin\theta_B=d/L$, $\mathcal{L}=L$, $u_t=0$, and Eqs. (63) and (64) reduce to Eq. (57) derived earlier. Another simple case is when the isolated vortex lines are trapped by the twin planes (the low vortex density): In this limit the free segments of the vortex lines between the twin boundaries are straight, $\langle\sin\theta\rangle=\sin\theta_0=d/\mathcal{L}$ (but $\mathcal{L}\neq L$!) and $u_t=d(\cot\theta_B-\cot\theta_0)$. Then

$$\rho_{\parallel}=\rho_t\sin^2(\theta_j-\theta_B)\frac{\sin\theta_0}{\sin\theta_B+(\rho_t/\rho_{tw})\sin(\theta_0-\theta_B)}\ ,$$

$$\rho_{\perp}=\rho_{Bt}\sin(\theta_j-\theta_B)\frac{\sin\theta_B}{\sin\theta_B+(\rho_t/\rho_{tw})\sin(\theta_0-\theta_B)}\ . \tag{65}$$

In the lock-in phase, $\theta_B=0$ and the Hall effect is absent since the vortex motion is guided by the twin boundaries:[28]

$$\rho_{\parallel}=\rho_{tw}\sin^2\theta_j,\quad \rho_{\perp}=0\ . \tag{66}$$

VIII. CONCLUSIONS

The continuum electrodynamics of the type-II superconductor in the mixed state has been developed to study pinning by parallel twin boundaries in a Y-Ba-Cu-O single crystal. The theory shows that the effect of pinning is screened at the distance of the distortion screening length from the twin boundaries, but the pinning onset weakly depends on the magnitude of the external magnetic field. This screening is a manifestation of the long-range interaction between vortices, as the Debye screening is a result of the long-range Coulomb interaction in a plasma. The distortion screening is also important for the position of the transition line between the lock-in phase (the vortices are completely trapped by the twin boundaries) and the pinning phase (the vortices are partially trapped by the twin boundaries).

The magnetic torque and all components of the resistance for a single crystal with parallel twin domains in the magnetic field rotating in the a-b plane have been studied. The resistance has been calculated within the phenomenological approach which assumes the dynamic parameters of vortices inside the twin domains and vortices completely trapped by twin boundaries to be known. The theory predicts how the resistance should vary when the external magnetic field is rotated in the a-b plane. It has been shown that the Hall component of the resistance is especially important for studying the phase diagram.

ACKNOWLEDGMENTS

An impetus to this work was done by discussion of the twin-boundary pinning with G. W. Crabtree. The author is also very much indebted to S. Dorogovtsev and N. Kopnin for interesting discussions of the results of the work.

[1]D. Deutscher and K. A. Müller, Phys. Rev. Lett. **59**, 1745 (1987).
[2]L. A. Vinnikov, L. A. Gurevich, G. A. Emel'chenko, and Yu. A. Osip'yan, Pis'ma Zh. Eksp. Teor. Fiz. **47**, 109 (1988) [JETP Lett. **47**, 131 (1988)].
[3]G. J. Dolan, G. V. Chandrashekar, T. R. Dinger, C. Feild, and F. Holtzberg, Phys. Rev. Lett. **62**, 827 (1989).
[4]L. J. Swartzendruber, A. Roitburd, D. L. Kaiser, F. W. Gayle, and L. H. Bennett, Phys. Rev. Lett. **64**, 483 (1990); **64**, 2962 (1990).
[5]W. K. Kwok, U. Welp, G. W. Crabtree, K. G. Vandervoort, R. Hultscher, and J. Z. Liu, Phys. Rev. Lett. **64**, 966 (1990).
[6]G. W. Crabtree, W. P. Kwok, U. Welp, J. Downey, S. Fleshler, and K. G. Vandervoort, Physica C **185-189**, 282 (1991).
[7]G. Blatter, J. Rhyner, and V. M. Vinokur, Phys. Rev. B **43**, 7826 (1990).
[8]H. E. Hall, Adv. Phys. **9**, 89 (1960).
[9]I. L. Bekarevich and I. M. Khalatnikov, Zh. Eksp. Teor. Fiz. **40**, 920 (1961) [Sov. Phys. JETP **13**, 643 (1961)].
[10]E. L. Andronikashvili, Yu. G. Mamaladze, S. G. Matinjan, and J. S. Tsakadze, Usp. Fiz. Nauk **73**, 3 (1961) [Sov. Phys. Usp. **4**, 1 (1961)].
[11]E. B. Sonin, Rev. Mod. Phys. **59**, 87 (1987); Physica B **178**, 106 (1992).
[12]A. A. Abrikosov, M. P. Kemoklidze, and I. M. Khalatnikov, Zh. Eksp. Teor. Fiz. **48**, 765 (1965) [Sov. Phys. JETP **21**, 506 (1965)].
[13]P. Mathieu and Y. Simon, Europhys. Lett. **5**, 67 (1988); see also T. Hocquet, P. Mathieu, and Y. Simon, Phys. Rev. B **46**, 1061 (1992).
[14]E. B. Sonin, A. K. Tagantsev, and K. B. Traito, Phys. Rev. B **46**, 5830 (1992).
[15]E. B. Sonin, Zh. Eksp. Teor. Fiz. **70**, 1970 (1976) [Sov. Phys. JETP **43**, 1027 (1976)].
[16]E. B. Sonin, Y. Kondo, J. S. Korhonen, and M. Krusius, Europhys. Lett. **22**, 125 (1993); M. Krusius, Y. Kondo, J. S. Korhonen, and E. B. Sonin, Phys. Rev. B **47**, 15 113 (1993).
[17]D. Feinberg and C. Villard, Phys. Rev. Lett. **65**, 919 (1990).
[18]W. K. Kwok, U. Welp, V. M. Vinokur, S. Fleshler, J. Downey, and G. W. Crabtree, Phys. Rev. Lett. **67**, 390 (1991).
[19]S. S. Maslov and V. L. Pokrovsky, Pis'ma Zh. Eksp. Teor. Fiz. **53**, 614 (1991).
[20]B. I. Ivlev and N. B. Kopnin, J. Low Temp. Phys. **77**, 413 (1989).

[21]J. R. Clem, M. W. Coffey, and Z. Hao, Phys. Rev. B **44**, 2732 (1991).
[22]E. B. Sonin (unpublished).
[23]R. J. Zieve, Yu. Mukharsky, J. D. Close, J. C. Davis, and R. E. Packard, Phys. Rev. Lett. **68**, 1327 (1992).
[24]L. N. Bulaevskii, M. Ledvij, and V. G. Kogan, Phys. Rev. Lett. **68**, 3773 (1992).
[25]Y.-Q. Song, W. P. Galperin, L. Tonge, T. J. Marks, M. Ledvij, V. G. Kogan, and L. N. Bulaevskii, Phys. Rev. Lett. **70**, 3127 (1993).
[26]S. A. Solin, N. Garcia, S. Vieira, and M. Hortal, Phys. Rev. Lett. **60**, 744 (1988).
[27]E. B. Sonin and A. L. Kholkin, Fiz. Tverd. Tela **34**, 1147 (1992) [Sov. Phys. Solid State **34**, 610 (1992)].
[28]Ya. V. Kopelevich, V. V. Lemanov, E. B. Sonin, and A. L. Kholkin, Pis'ma Zh. Eksp. Teor. Fiz. **50**, 188 (1989) [JETP Lett. **50**, 212 (1989)].